Dynamic and Stable Populations of Microtubules in Cells

Eric Schulze and Marc Kirschner

Department of Biochemistry and Biophysics, University of California at San Francisco, San Francisco, California 94143-0448

Abstract. Using a new immunocytochemical technique, we have visualized the spatial arrangement of those microtubules in cells that are stable to biotin–tubulin incorporation after microinjection. Cells fixed at various periods of time after injection were exposed to antibody to biotinylated tubulin and several layers of secondary antibodies; these layers prevented reaction of biotin-containing microtubules with anti-tubulin antibodies. The microtubules that had not incorporated biotin–tubulin could then be stained with anti-tubulin and a fluorescent secondary antibody. In BSC1 cells, most microtubules in the cell exchange with a half-time of 10 min. A separate population of microtubules can be detected, using the above techniques, that are stable to exchange for 1 h or more; these have a characteristic pericentrosomal spatial arrangement as compared to the majority of dynamic microtubules. Unlike the dynamic microtubules, most of the stable microtubules are nongrowing. The average BSC-1 cell contains ~700 microtubules: ~500 growing at 4 μm min^{-1}, 100 shrinking at ~20 μm min^{-1}, and ~100 that are relatively more stable to exchange. The potential significance of these stable microtubules is discussed.

A fundamental problem in cell biology is the asymmetric placement of components within the cell. The cytoskeleton and, in particular, microtubules are thought to play an important role in cell asymmetry, since their depolymerization often leads to withdrawal of cell processes, inhibition of cell movement, and displacement of the nucleus and cell organelles. In many cells, microtubules have an overall asymmetric distribution. Polarity can also be achieved if the distribution is symmetric but some microtubules in the cell are differentiated from others. Recently, support for spatial differentiation of microtubules has come from the study of posttranslational modifications of tubulin, such as detyrosination and acetylation (Gunderson et al., 1984; LeDizet and Piperno, 1986). Such modifications have been shown to occur on a spatially distinct subpopulation of microtubules in the cell.

A simple explanation for the differentiation of neighboring microtubules is that microtubules in the cell differ in age (Kirschner and Mitchison, 1986). In the case of detyrosination, the available evidence supports the view that older microtubules could rather uniformly accumulate posttranslational changes. This pattern of modification of neighboring microtubules is consistent with the pattern of microtubule growth expected from the model of dynamic instability in vitro (Mitchison and Kirschner, 1984*a*, *b*; Horio and Hotani, 1986).

Recently, we have studied the pattern and rate of microtubule growth in fibroblast cells by injecting cells with biotin-labeled tubulin and observing the pattern of new assembly (Schulze and Kirschner, 1986). These experiments and others involving incorporation of fluorescein-labeled tubulin and photobleaching (Saxton et al., 1984; Soltys and Borisy, 1985) suggest that microtubules turnover and grow very rapidly in vivo, displaying a pattern of nucleation, growth, and rapid shrinkage, which leads to replacement of microtubules one by one. Most microtubules followed this pattern of replacement and were found to have a half-life of 5–10 min. However, some microtubules were more stable and unlabeled microtubule segments could still be seen at 1–6.5 h, although all microtubules exchanged by 10 h.

In this report we examine in more detail the turnover, number, and spatial distribution of stable microtubules in two cell lines. We demonstrate, by means of a new immunocytochemical technique, that these stable microtubules are generally continuous nongrowing polymers with a distribution distinct from that of the dynamic population of microtubules. We also report the results of a more detailed analysis of the dynamic microtubule population. These data on the number and fraction of growing microtubules, along with our better understanding of stable microtubules, allows us to model, in general terms, the behavior of microtubules in an interphase cell. How the various microtubule classes arise from the presumably homogenous dynamic microtubule population, and their possible functional significance are also discussed.

Materials and Methods

Materials

N-Hydroxysuccinimidyl biotin was from Polysciences, Inc. (Warrington, PA); rabbit anti-biotin antibody was from Enzo Biochem, Inc. (New York, NY). Mouse monoclonal anti-β-tubulin was a kind gift of Dr. S. H. Blose

(Protein Databases, Inc., Huntington Station, NY). Unlabeled, and rhodamine- and fluorescein-labeled secondary antibodies were from Cappel Laboratories (CooperBiomedical Inc., Malvern, PA). Texas red-labeled rat anti-mouse antibody was from Accurate Chemical & Scientific Corp. (Westbury, NY). Nocodazole was from Aldrich Chemical Co. (Milwaukee, WI).

Tubulin Preparation

Phosphocellulose-purified tubulin was prepared from bovine brains by a modification of the procedure of Weingarten et al. (1975) as described in Mitchison and Kirschner (1984*a*, *b*). Protein concentrations were determined by the method of Bradford (1976), using BSA as a standard.

Preparation of Biotinylated Tubulin

Biotinylated tubulin was prepared as described in Kristofferson et al. (1986) and Mitchison and Kirschner (1985) with modifications for microinjection as in Schulze and Kirschner (1986).

Cell Culture

African Green monkey kidney fibroblasts (BSC1) (a kind gift of U. Euteneuer, University of California at Berkeley) were grown in DME supplemented with 10% FCS (Gibco, Grand Island, NY). Human retinoblastoma cells (SKNSH) (a kind gift of Manfred Schwab, University of California at San Francisco) were grown in RPMI 1640 with 10% FCS (Bluestein, 1978). For microinjection studies, the cells were trypsinized off tissue culture dishes and replated onto 1-in-diameter poly-D-lysine-coated coverslips. BSC1 cells were allowed to settle for 1 d before use; SKNSH cells were allowed to settle for 1 d, and differentiated in 30 μg/ml retinoic acid for ~3 d before use.

Microinjection

Cells on coverglasses were placed in a thermostatted microinjection chamber at 37°C as described in Schulze and Kirschner (1986). The chamber was then placed on a Zeiss ICM 405 inverted microscope allowing direct access from above. The cells were then pressure microinjected using the technique of Graessman and Graessman (1976). Microinjection needles were drawn out to ~0.5–1 μm diameter tips using a micropipette puller model 720 equipped with patch clamp adapter 728A (David Kopf Instruments, Tujunga, CA). We estimate that approximately one-tenth of a cell volume was typically injected (Graessman et al., 1980).

Antibody-blocking Technique

After injection of cells with 10 mg/ml biotin-tubulin, cells were allowed to incubate at 37°C in a CO_2 incubator for the desired period of time, from 5 min to 2 d. The cells were then washed with PBS for 2 s, then immersed in room temperature permeabilization buffer (80 mM Pipes, 5 mM EGTA, 1 mM $MgCl_2$, 0.5% NP-40) for 20 s, after which glutaraldehyde (0.5% final concentration) was added to the permeabilization buffer with gentle mixing. After fixation (10 min), the cells were washed for 10 s in PBs, before being treated for 6 min in PBS plus 1 mg/ml $NaBH_4$ to quench the glutaraldehyde. Cells were then washed with a solution of PBS plus 0.1% Triton X-100 (antibody buffer) and incubated in the antibody buffer for 40 min. To stain the cells for stable microtubules, in brief, one follows an anti-biotin antibody with a series of four secondary antibodies. This essentially forms an immunoprecipitate on microtubules which have incorporated any biotin-tubulin. Reacting the cell with anti-tubulin then reveals only the remaining non-biotin-tubulin-containing microtubules; i.e., the stable microtubules. In this protocol, all antibodies are used at room temperature at concentrations of 5 μg/ml. Between each successive incubation with antibody, the cells are washed five times, and incubated for 5 min with antibody buffer. The primary rabbit anti-biotin is used for 1 h, followed by fluorescein-labeled goat anti-rabbit (40 min), fluorescein rabbit anti-goat (40 min), unlabeled goat anti-rabbit (40 min), and unlabeled rabbit anti-goat antibodies (40 min). One can use labeled secondaries for all the steps, but we found that this significantly decreases the signal-to-noise ratio. The above steps accomplish the visualization and blocking of the dynamic (biotin-tubulin-containing) microtubules leaving the rest of the microtubules essentially untouched. The remaining stable microtubules can then be visualized using a mouse monoclonal anti-β-tubulin (30 min) followed by an appropriate secondary; we have used both rhodamine labeled sheep anti-mouse or Texas red-labeled rat anti-mouse antibodies (30 min). Mounting and photography were carried out as in Schulze and Kirschner (1986). The use of hypersensitized technical Pan 2415 film (Eastman Kodak Co., Rochester, NY) with its extremely fine grain, made possible the accurate analysis of highly magnified images.

Nocodazole Experiments

SKNSH cells were injected with 10 mg/ml biotin-tubulin, and incubated for 1 h in a 37°C tissue culture incubator. The cells were then incubated in either 1 μg/ml or 10 μg/ml nocodazole 37°C in tissue culture media for either 2 or 10 min, respectively. The cells are then immersed into a modified permeabilization buffer (80 mM Pipes, 5 mM EGTA, 1 mM $MgCl_2$, 0.5% NP-40, 20% glycerol by volume) for 45 s at room temperature. The addition of glycerol to the permeabilization buffer helps stabilize the microtubules during the slightly longer permeabilization necessary to remove the large pool of free tubulin in these nocodazole-treated cells. Glutaraldehyde (0.5%) is then added with gentle mixing, and the cells are fixed for 10 min followed by the above described antibody-blocking technique.

Cell Area Measurement and Average Microtubule Length Measurement

Negatives of microinjected cells were projected onto a GITCO (Rockville, MD) digitizing pad interfaced to an IBM PC. The perimeter of the cell was traced, and area calculated using the supplied software. The length of growing microtubules was measured from negatives of three cells microinjected and incubated for short times (2 min). The length of each growing microtubule was approximated by measuring from a defined point in the cell center to the end of a growing segment. The digitized lengths were stored on an IBM PC for subsequent statistical analysis.

Microtubule Number and Percent of Growing Microtubules at the Periphery

Microtubule segments were counted by using 8 × 10-in enlargements of cells injected with biotin-tubulin and incubated for short times (5 min). The percent of microtubules growing at the periphery was calculated from injected cells with short incubations which were prepared using either the antibody-blocking technique, or standard immunofluorescence techniques. High magnification pictures were printed of both the anti-tubulin and anti-biotin staining; all unambiguous ends were recorded as either biotin-tubulin ends, or unexchanged ends, from which we calculated the fraction of microtubule ends with biotin segments.

Results

Visualization of Stable Microtubules

We have previously described the existence of a minority class of microtubules in BSC1 cells that was more stable to exchange with free tubulin than the majority of microtubules. These microtubules were identified in cells which had been injected with biotin-tubulin and incubated for 2 h before fixation. The unexchanged segments could be identified only by comparing the pattern of all the microtubules stained with anti-tubulin with the microtubules that had incorporated biotin and been stained with anti-biotin. Since after 2 h, most microtubules were stained with both anti-biotin and anti-tubulin, the overall spatial organization of the unexchanged segments was difficult to discern. In addition, the unexchanged microtubules often seemed to be situated close to the centrosome where microtubule density was the highest, making it impossible to trace unambiguously an unexchanged segment for any appreciable length. To visualize these unexchanged microtubules, we needed to be able to look at the unincorporated microtubule segments directly. To do this, we developed a technique whereby we blocked the anti-tubulin antibody from reacting with microtubules that had incorporated significant amounts of biotin-tubulin; the remaining unexchanged microtubules, which were stable to

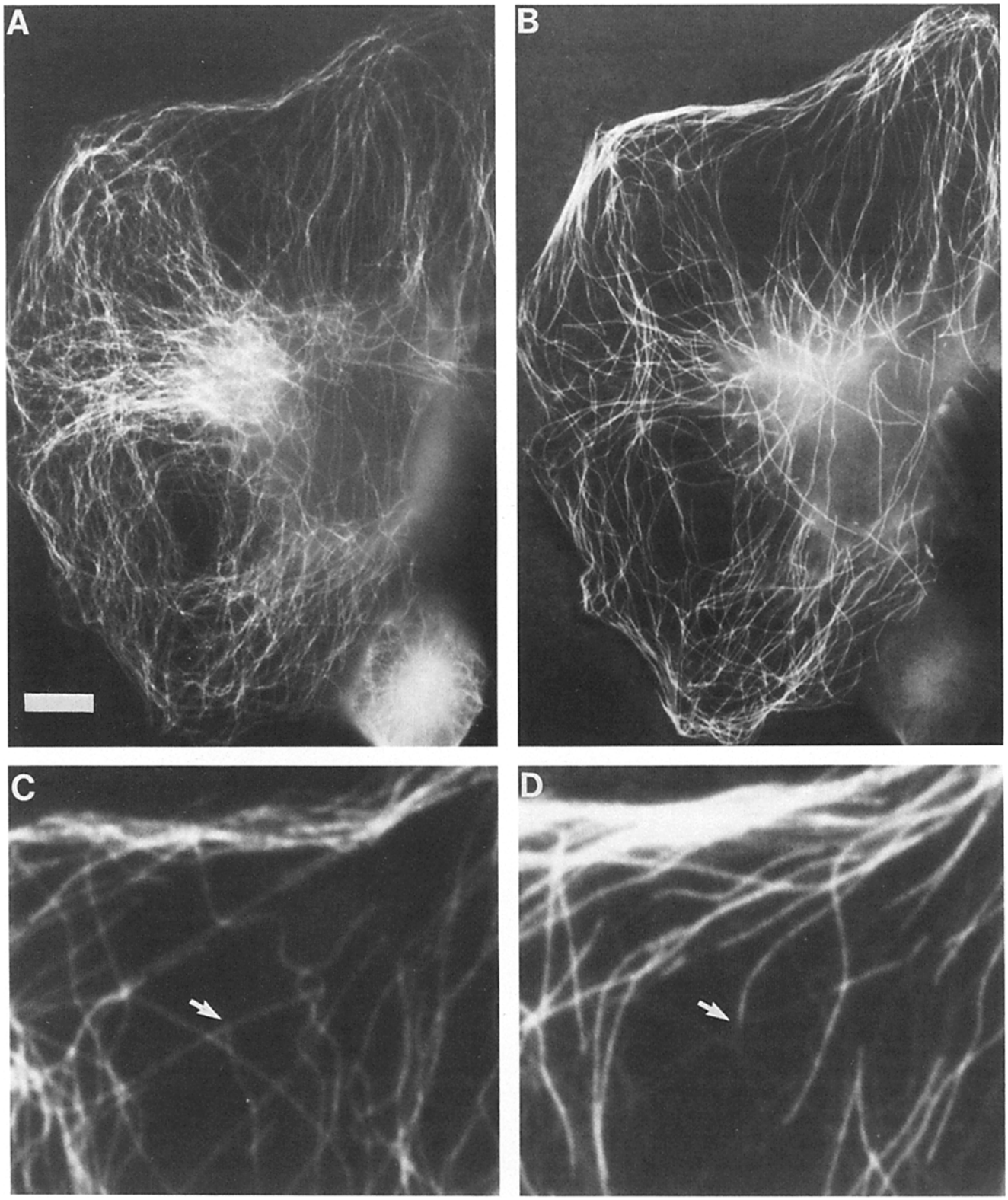

Figure 1. Immunofluorescence micrograph of a cell injected with biotin-tubulin and incubated for 5 min before preparation using the antibody-blocking technique. (*A*) Fluorescein anti-tubulin staining showing only non-biotin-tubulin-containing microtubules. (*B*) Rhodamine anti-biotin staining showing only exchanged segments. (*C*) Higher (3.5-fold) magnification view of anti-tubulin staining in the upper middle part of the cell. (*D*) Higher magnification view of anti-biotin staining of the same area as in *C*. Arrows point to point of transition between unexchanged and exchanged segments of the same microtubule. Bar, 10 μm.

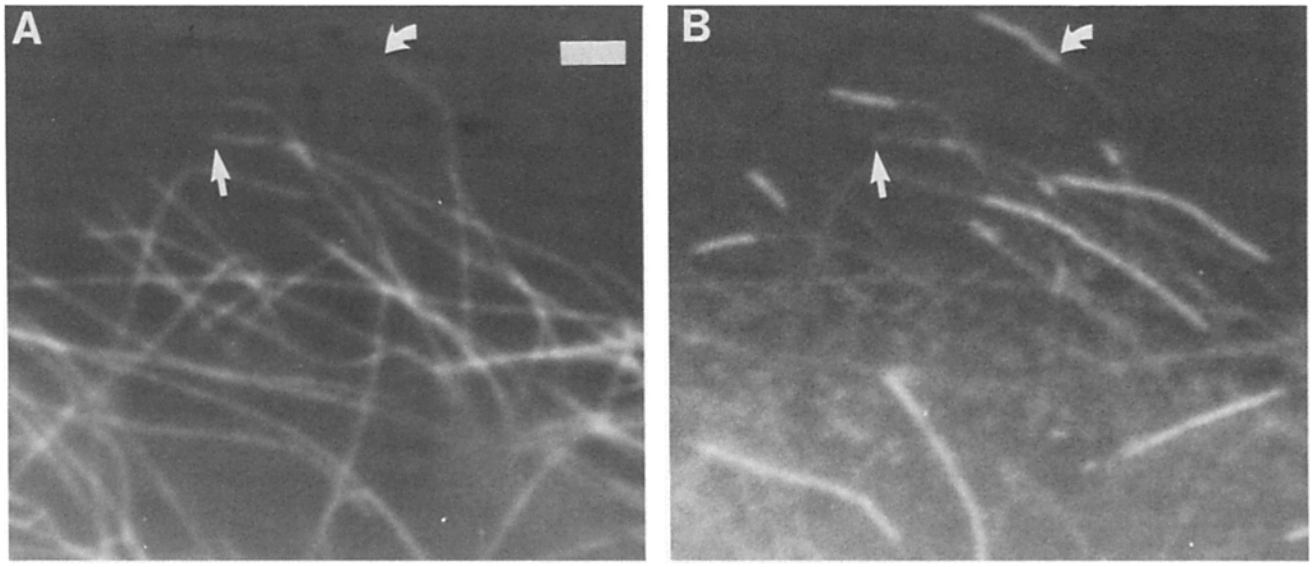

Figure 2. High magnification view of a small area of a BSC1 fibroblast injected with biotin-tubulin and incubated for 2 min before preparation using the antibody-blocking technique. (*A*) Anti-tubulin staining of only the unexchanged microtubule segments. (*B*) Anti-biotin staining of only the biotin-tubulin-containing segments (i.e., areas of new growth). Thin arrows point to a microtubule end without visible exchange; curved arrows point to segment of new growth at a microtubule end. Bar, 2 μm.

exchange during the time between injection and fixation, were revealed by reacting with an anti-tubulin antibody.

The method for visualization of these unexchanged microtubules is as follows: a cell is first injected with biotin-labeled tubulin and then allowed to incubate for a given period of time to allow for biotin-tubulin incorporation. The cell is then permeabilized, and fixed for immunofluorescence. The first antibody used is a rabbit anti-biotin polyclonal antibody. This antibody will react with only those microtubules that have incorporated biotin-tubulin, i.e., those that have polymerized during the incubation period after injection of the biotin-tubulin. The second and third antibodies are fluorescently labeled goat anti-rabbit and fluorescently labeled rabbit anti-goat antibodies, respectively. These antibodies allow the visualization of the microtubules that had incorporated biotin-tubulin. Next, the fixed cells are reacted with unlabeled goat anti-rabbit and rabbit anti-goat antibodies. These steps essentially form an immunoprecipitate on the biotin-tubulin-containing microtubules, preventing further reaction with anti-tubulin antibodies. The cells are next reacted with a mouse monoclonal anti-tubulin antibody, which reacts now only with microtubules that have not been covered by the immunoprecipitate formed by the previous five antibodies; these are the microtubules that have not incorporated biotin-tubulin. The last step is to use a fluorescently labeled rat anti-mouse antibody to visualize the microtubules stained by the monoclonal mouse anti-tubulin antibody. This method distinguishes microtubules solely on the basis of whether they have incorporated significant amounts of biotin-tubulin. At a molar ratio of ~1 mol bio-

Table I. Percent of Microtubules Showing Biotin-Tubulin Segments at the Cell Periphery

Cell No.	Microtubules counted	Growing microtubules
	n	%
1	91	86
2	55	78
3	39	87
4	40	65
Total	225	80

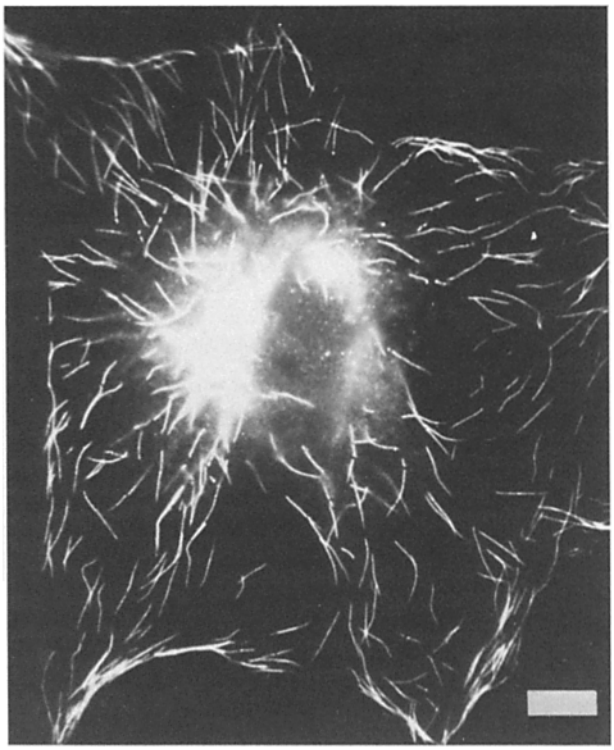

Figure 3. Standard immunofluorescence micrograph of anti-biotin staining in a BSC1 cell injected with biotin-tubulin and incubated for 2 min. The number of MT segments counted in this cell is 515. Bar, 10 μm.

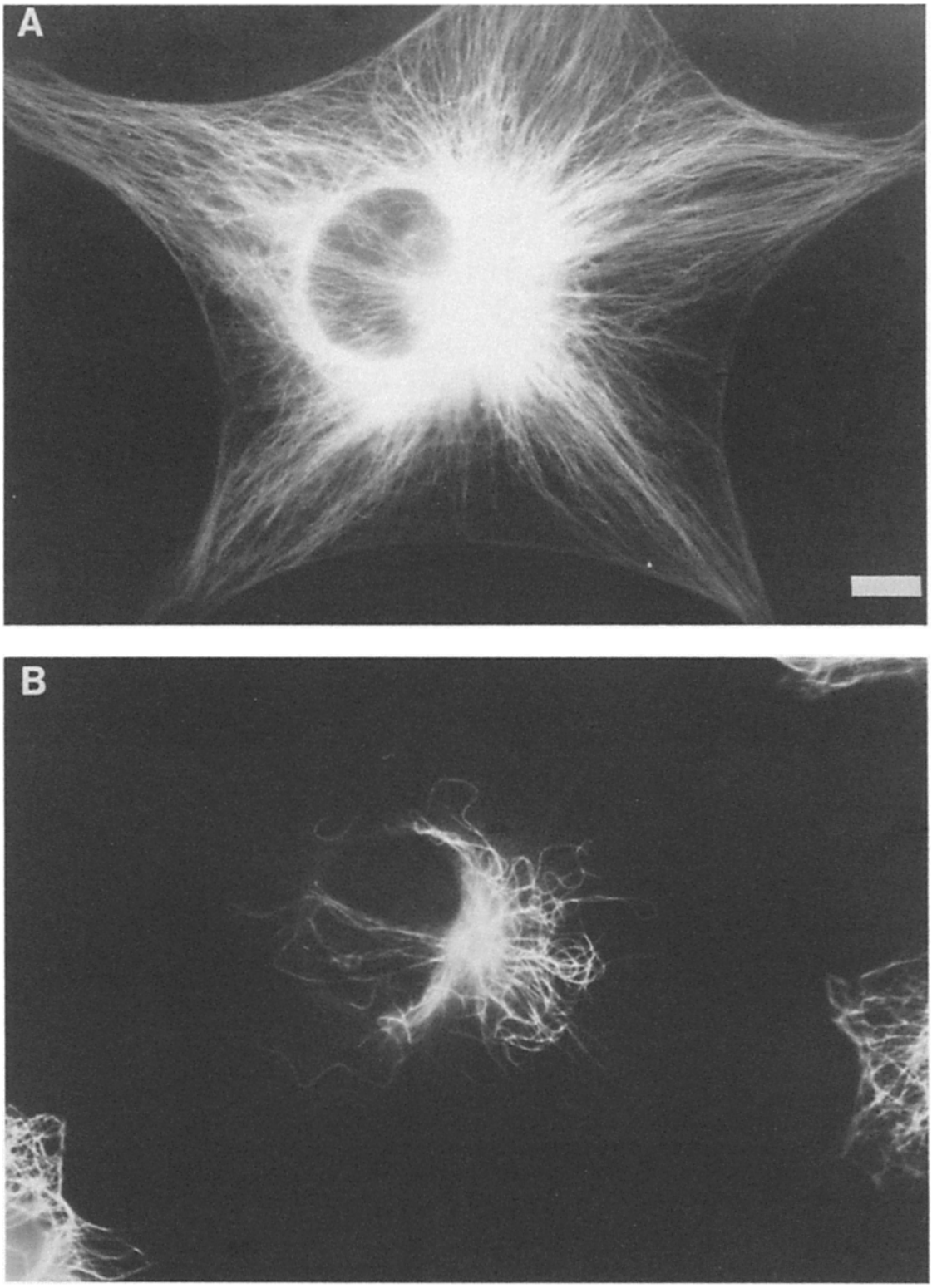

Figure 4. Immunofluorescence micrograph of BSC1 cell injected with biotin–tubulin and incubated for 2 h before preparation using the antibody-blocking technique. (*A*) Anti-biotin staining showing the exchanged (dynamic) microtubules. (*B*) Anti-tubulin staining revealing the unexchanged (stable) microtubules. Bar, 10 μm.

tin–tubulin to 10 mol of unmodified tubulin, four layers of antibody are sufficient to block reaction to subsequent addition of anti-tubulin.

Fig. 1 is an example of the use of this technique on BSC1, African green monkey kidney cells after a rather short (5-min) incubation. During the 5-min incubation, there has been extensive assembly of biotin–tubulin-containing subunits into microtubules shown in Fig. 2 *B* in the rhodamine channel. Fig. 1 *A* is the fluorescein (anti-tubulin) channel showing the microtubules that have not incorporated biotin–

tubulin during the incubation. Close examination of these two pictures shows that they are in fact non-overlapping.

Fig. 1, *C* and *D*, shows that on the level of single microtubules the distributions are complementary as well as non-overlapping. Shown here is a magnified region of the upper middle portions of Fig. 1, *A* and *B*. The micrograph of the anti-biotin staining (Fig. 1 *D*) has been overexposed to allow some bleed-through of the fluorescein image as observed with the broad band fluorescence filters. (Note this is due to bleed-through rather than cross-reactivity of the antibody as demonstrated in control experiments with single antibody staining). As one can see, several microtubules in the pictures are chimeric, abruptly changing (note the arrow) from fluorescein to rhodamine.

This technique can be used to evaluate the fraction of microtubules near the cell periphery that exhibit growth at their ends after short incubation times. Fig. 2, *A* and *B*, shows complementary images of anti-tubulin versus anti-biotin staining of a peripheral region of a cell 2 min after injection. All new segments in Fig. 2 *B* can be seen to be extensions of pre-existing microtubules. Some segments clearly have no discernible growth. One of these microtubules is indicated by the arrows in Fig. 2, *A* and *B*. As shown in Table I, 80% of all microtubules near the cell periphery have incorporated new subunits within 2 min after injection. By evaluating pictures of cells incubated for short time points using either the blocking technique or the standard immunofluorescence techniques (Fig. 3), one can also count the total number of microtubules growing at any one time throughout the whole cell. For the cell pictured in Fig. 3, the number of growing microtubules is 515. As shown in Table II, the number of growing segments increases roughly linearly with the measured area of the cell. The average number of growing microtubules in cells with areas between 2.7 and 13.1 $\times$ 10^3 μm^2 is 471. The median area of cells injected is 5.4 $\times$ 10^3 μm^2 and such a cell would have 446 growing microtubules.

Although these experiments at short incubations are facilitated by using the antibody-blocking method to obtain complementary images of new and old subunit incorporation, the critical use of the antibody-blocking technique is to demonstrate microtubules stable to exchange at long periods of time. Athough a majority of microtubules in the cell (roughly estimated at 80%) have exchanged by 15 min, appreciable numbers have not incorporated subunits at 2 h. This can be seen clearly at 2 h in Fig. 4 *B* where the stable microtubules represent an appreciable minority population when compared to the dynamic population in Fig. 4 *A*. In the simplest possible model, all microtubules in the cell would have identical stability. In a cell of 700 microtubules (see Discussion) we would estimate that fewer than 10 unlabeled microtubules should remain at 1 h and none should be present at 2 h. Since the unexchanged population at 2 h in Fig. 4 is much larger than expected, we shall refer to these unexchanged polymers as stable microtubules, although it should be remembered that this is strictly an operational definition. Fig. 4, *A* and *B*, clearly demonstrates the difficulty there would be in visualizing unexchanged microtubules by subtracting the dynamic population from the total. These stable microtubules would be lost amongst the masses of dynamic microtubule near the cell center.

Table II. Number of Growing Microtubules in 10 BSC1 Cells

Cell No.	Dynamic ends	Area
	n	μm^2
1	324	2,668
2	273	3,015
3	492	4,344
4	421	4,715
5	485	4,840
6	539	6,055
7	481	7,188
8	462	7,351
9	615	8,600
10	620	13,125

The total number of growing microtubules (MTs) was estimated for cells injected with biotin-tubulin from 40 s to 2 min using the standard double-label technique. Both the number of segments and the area of the cell is given. Total number increases with size. The equation of the least squares fitted line for number of microtubules versus area of the cell is as follows: number of MTs = area (μm^2) $\times$ 2.9 $\times$ 10^{-2} (MTs/μm^2) + 289 MTs, with a correlation coefficient of 0.82.

Spatial Distribution of Stable Microtubules

It was clear from the first few experiments that the stable microtubules revealed by the antibody-blocking technique exhibited a different intracellular distribution from that of the dynamic microtubules. When we looked at the distribution in BSC1 fibroblasts and SKNSH human retinoblastoma cells, we found that although both cell lines exhibit heterogeneity in both morphology and size, nevertheless there were several common characteristics of the distribution of stable microtubules in both cell types. Fig. 5 is an example of a very large BSC1 fibroblast injected with biotin-tubulin 1 h before preparation using the antibody-blocking technique (dynamic microtubules in Fig. 5 *A*; stable microtubules in Fig. 5 *B*). Comparison with Fig. 4 is instructive. Apart from the most obvious difference, there being many more stable microtubules at 1 h in the larger cell than at 2 h with the smaller, the similarities in both distribution and morphology of the stable microtubules is quite striking, and in fact holds true in most cells studied. In both cells, the stable microtubules are curly, or kinky, compared to the dynamic microtubules which are generally straight. The stable microtubules are also seen to cluster around the cell center close to the centrosome and Golgi apparatus. In addition, the stable microtubules rarely extend to the cell periphery, as opposed to the dynamic microtubules many of which reach the cell's edge. The stable microtubules also tend to be more three-dimensional, moving in and out of the plane of focus in which the vast majority of dynamic microtubules are seen.

To see whether this distribution was restricted to BSC-1 cells, we examined a human retinoblastoma cell line (SKNSH) as shown in Fig. 6 1 h after injection. Again, stable microtubules are curly, clustered around the cell center, and generally do not enter peripheral areas of the cell.

Turnover of Stable Microtubules

Ideally one would like to measure the stability of each individual microtubule in a cell. In practice, the injection procedure allows one to follow a cohort of microtubules that had not exchanged with the free tubulin after injection. This co-

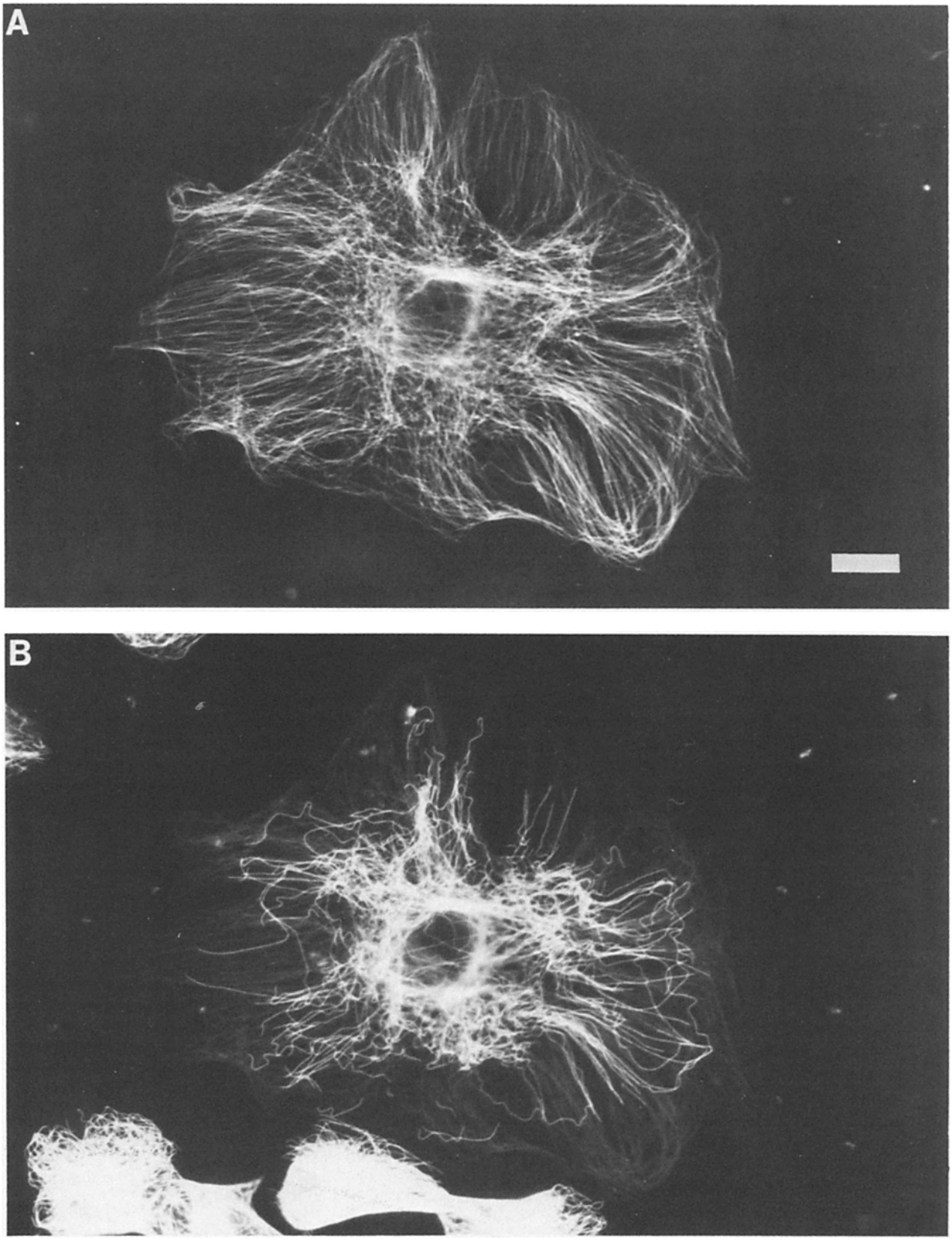

Figure 5. Immunofluorescence micrograph of a very large BSC1 cell injected with biotin-tubulin and incubated for 1 h before preparation using the antibody-blocking technique. (*A*) Anti-biotin staining showing the dynamic microtubules. (*B*) Anti-tubulin staining revealing the stable microtubules. Bar, 20 μm.

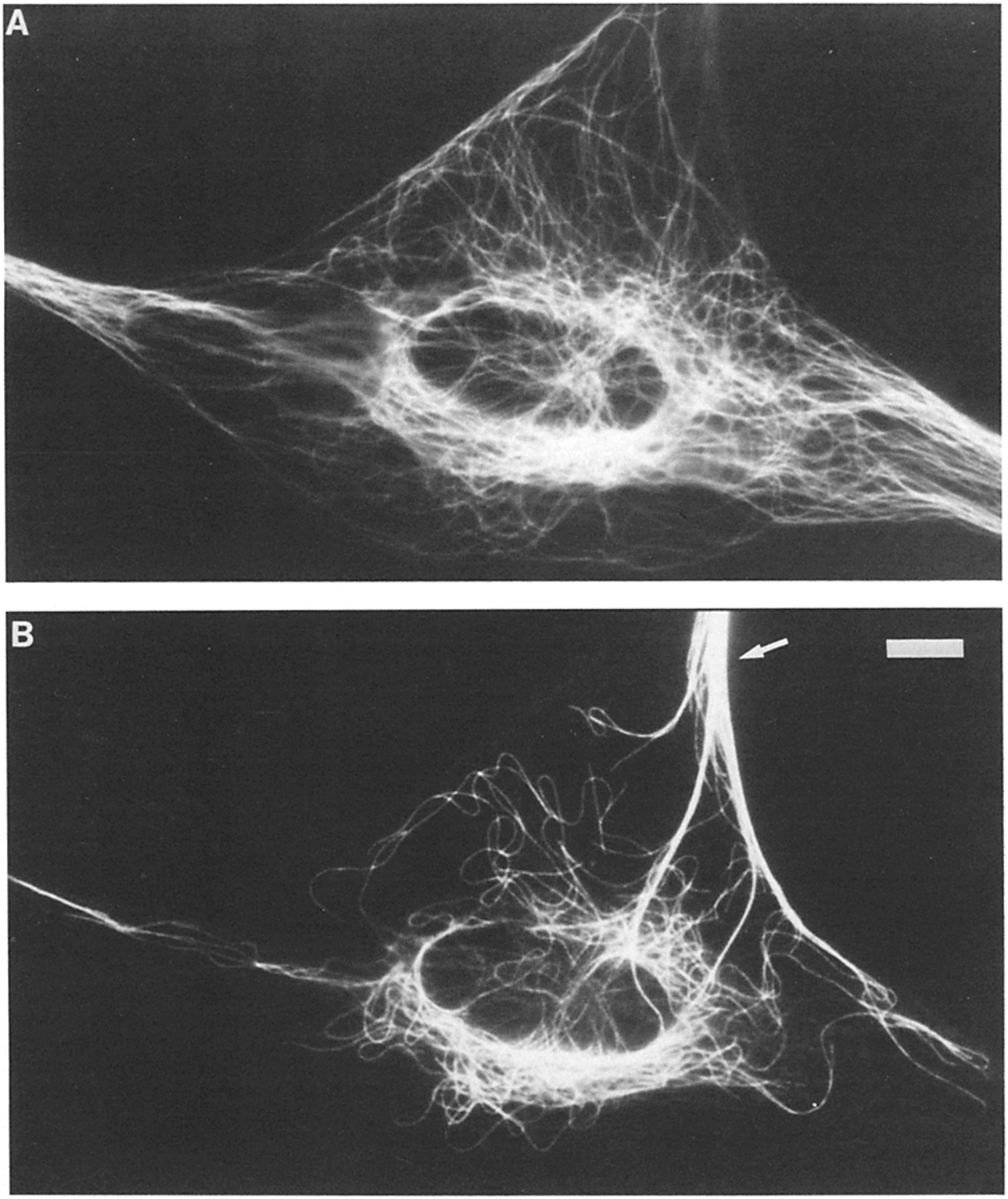

Figure 6. Immunofluorescence micrograph of an SKNSH cell injected with biotin–tubulin and incubated for 1 h before preparation using the antibody-blocking technique. (*A*) Anti-biotin staining showing the dynamic microtubules. (*B*) Anti-tubulin staining revealing the stable microtubules. Arrow points to process extended from a neighboring uninjected cell. Bar, 10 μm.

hort will contain a population of microtubules with a distribution of stabilities, and this distribution will shift towards greater stability with time after injection. Thus, any simple analysis will only approximate the number and stability of microtubules in the cell. During the first few minutes after injection (Fig. 1), the unlabeled microtubule population contains a large number of dynamic microtubules. However, by 1 h, (Figs. 5 and 6), the number of dynamic microtubules left in the stable population should be small (assuming a half-time of 10 min) and the stable population will be enriched

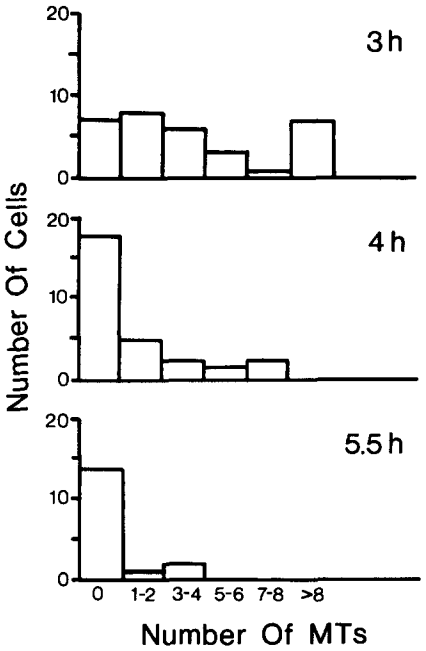

Figure 7. Histograms of the number of cells with the indicated number of stable microtubules versus time of incubation. The number of stable microtubules was determined during viewing under the microscope to avoid the problem of microtubules going in and out of the plane of focus. Only cells with areas between 1,000 and 6,000 μm^2 were plotted. The average number of microtubules per cell was 4.16, 1.17, and 0.53 at 3, 4, and 5.5 h of incubation before preparation using the antibody-blocking technique.

in microtubules that are more stable. The number of unexchanged microtubules declines steadily and by 3 h, it is usually easy to count them.

Fig. 7 shows histograms of the number of stable microtubules (counted through the microscope to avoid problems with microtubules moving in and out of the plane of focus) per cell at 3, 4, and 5.5 h. At 2 h, the number is too great to count. In these histograms, we have included data from cells that have an area up to 6,000 μm^2. A few much larger cells have many more stable microtubules (for example, whereas the average number of unexchanged microtubules at 3 h for the cells in the histogram below 6,000 μm^2 is 4.2 microtubules/cell, for cells between 9,000 and 16,000 μm^2, there is an average of 28 stable microtubules/cell). These large cells represent ~10% of the cell population and will not be considered. There is considerable heterogeneity in the population at 3 h, but by 6.5 h, virtually all of the microtubules not containing biotin-tubulin in the cells have disappeared. Stable microtubules are therefore not permanently stable but only relatively more stable than the dynamic population. Although their number declines with time, the average length of the remaining microtubules does not appear to change much with time.

We have also looked carefully to see how many stable microtubules are in the process of growing. This is difficult because most of the stable microtubules end near the cell center where the density of biotin-labeled segments is very high and hence it is difficult to see unambiguously if there is a biotin-labeled segment at the end of a stable microtubule. However, we have looked at 37 identifiable ends of stable microtubules (in three cells incubated for 40 min, 1.5 h, and 2 h) and found that only 7 (~20%) showed any biotin segments at their ends. This was in contrast to the 80% of total microtubules which showed incorporation in short pulses (Table I).

Relationship of Nocodazole Stability to Temporal Stability

It has been proposed that microtubules that are stable to nocodazole or colchicine represent a special subclass of microtubules in the cell (Behnke and Forer, 1967). Alternatively, it is possible that the very act of treating a cell with colchicine causes release of bound proteins and generates increased stability in the remaining microtubules. We have asked whether all microtubules that are stable to exchange are also particularly stable to nocodazole-induced depolymerization. To test this, SKNSH cells were microinjected with biotin-tubulin for 1 h, then exposed to either high (Fig. 8, *C* and *D*) or low (Fig. 8, *A* and *B*) concentrations of nocodazole for 10 min or 2 min, respectively, causing extensive depolymerization of the microtubule arrays; they were then stained for biotin content using the antibody-blocking technique. Two pairs of representative pictures show that qualitatively, nocodazole treatment causes a dramatic loss of both dynamic microtubules (Fig. 8, *A* and *C*) and stable microtubules (Fig. 8, *B* and *D*) when compared to untreated samples (Fig. 6). Whether stable microtubules are quantitatively more stable to nocodazole would be difficult to answer without extensive statistical analysis.

Discussion

Many cells, for example, neurons, are highly topographically differentiated and it seems reasonable to think that this differentiation is based, in part, on the spatial organization of the cytoskeleton. In this report, we have examined the spatial distribution of microtubules in terms of their kinetic properties. The high density of microtubules near the cell center and the inherent restricted resolution of the light microscope put limits on any subtractive technique for tracing chemically differentiated microtubules in the cell. For many purposes it is necessary to be able to look directly at each type of microtubule separately. The simple method presented here of using one antibody and layers of secondary antibodies to block the reactivity of another, generates a clear picture of the distribution of microtubules not containing biotin even in a sea of microtubules containing biotin. This method could be used in principle to distinguish any modifications of microtubules or other components of the cell or even to define whether two antibodies stain the same components, and it is especially needed when the structures are below the limit of resolution in the light microscope. We have also used this method successfully to distinguish tyrosinated tubulin and nontyrosinated tubulin with a single antibody to the tyrosinated protein and a general antibody to tubulin (Schulze, E., unpublished results).

The antibody-blocking method allows one to follow separately the appearance of new microtubules and the disappearance of old microtubules. The distributions of the old and new microtubules are non-overlapping (see Fig. 2). Such distributions are consistent with microtubules newly nucleated from the centrosome replacing microtubules that dis-

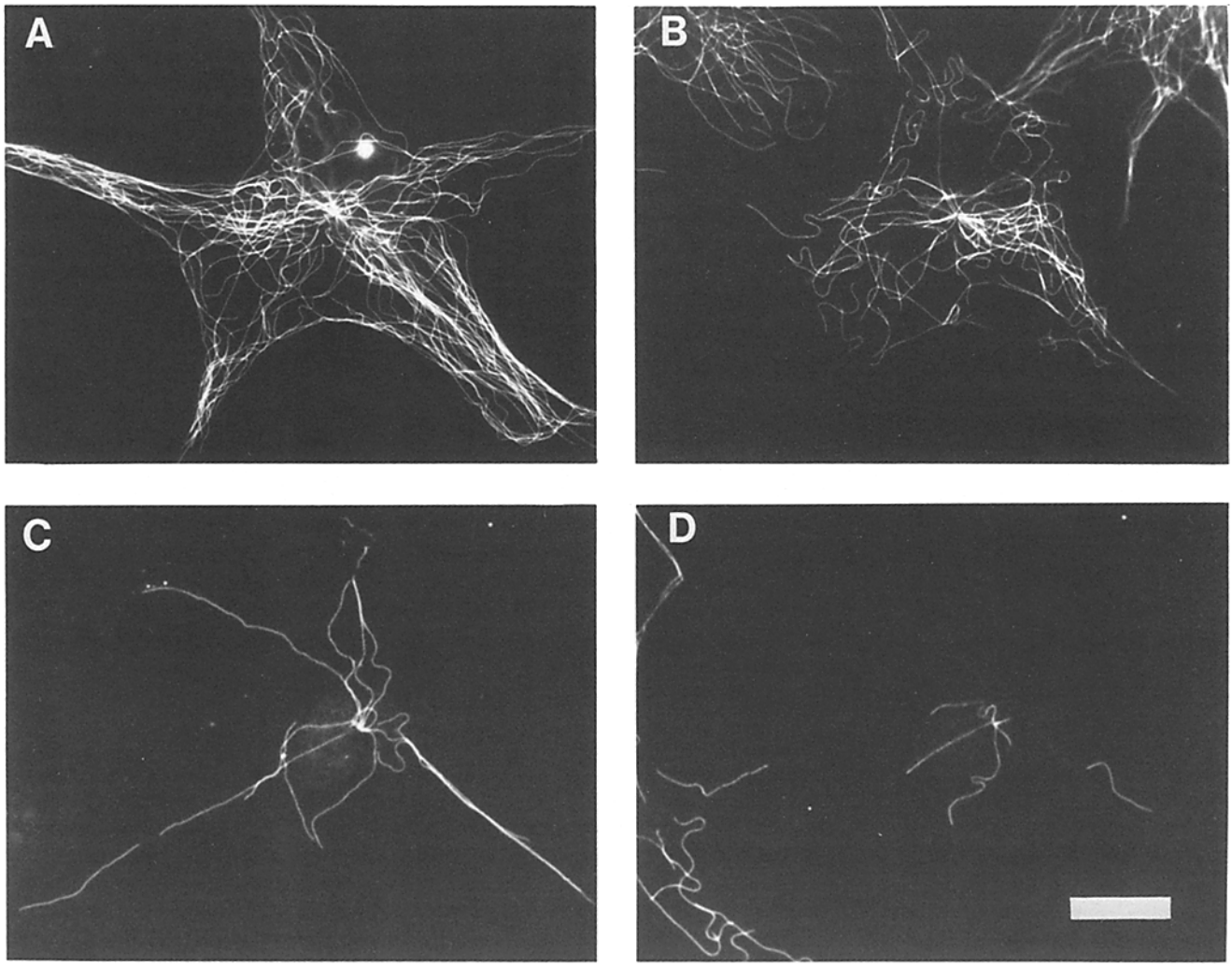

Figure 8. Immunofluorescence micrographs of two SKNSH cells injected with biotin–tubulin and incubated for 1 h before treatment with nocodazole and subsequent preparation using the antibody-blocking technique. (*A*) Anti–biotin staining of a cell treated with a low concentration of nocodazole (1 μg/ml for 2 min) showing the nocodazole-resistant dynamic microtubules. (*B*) Anti–tubulin staining of same cell depicting the nocodazole-resistant stable (non-exchanged) microtubules. (*C*) Anti–biotin staining of cell treated with a high concentration of nocodazole (10 μg/ml for 10 min) showing the nocodazole-resistant dynamic microtubules. (*D*) Anti–tubulin staining of the same cell revealing the nocodazole-resistant stable microtubules. Bar, 20 μm.

appear in their entirety. The number of biotin-containing microtubules increases with time and the number of unexchanged microtubules declines with time and hence the incorporation of biotin–tubulin into microtubules is not due to excess initiation of new microtubules but is caused by replacement of old microtubules with newly nucleated ones. This pattern of assembly has recently been interpreted in terms of the model of dynamic instability (Schulze and Kirschner, 1986; Kirschner and Mitchison, 1986; Mitchison and Kirschner, 1984*a*, *b*; Soltys and Borisy, 1985). As reported previously, new growth occurs throughout the cell at rates independent of the concentration of biotin–tubulin (Schulze and Kirschner, 1986). At short times all microtubule growth appears at the ends of existing microtubules and off the centrosome and hence there does not appear to be any spontaneous nucleation. We have also seen no examples of segmented microtubules (composed, for example, of an isolated stable segment jointed to two biotin segments or vice versa) and therefore find no evidence for microtubules that might have annealed in interphase BSC1 or SKNSH cells.

The half-time of microtubule turnover in BSC1 cells has been estimated by photobleaching experiments to be between 1.5 and 5 min (Saxton et al., 1984). From our experiments, we estimate a half-time of the dynamic population of ~10 min (Schulze and Kirschner, 1986). By 15 min, it is clear that a majority of microtubules have exchanged. Thus these two different methods give comparable results. If all microtubules in the cell had a half-time of 10 min, an average of 11 microtubules would be expected to remain after 1 h, and none after 2 h. The existence of many stable microtubules at 2 or even 3 h (Figs. 4–6) indicates that microtubules of greater stability than the majority population must exist in the cell.

The microtubules that have not exchanged subunits in 2 h have particular spatial characteristics. They are kinked and bent in three dimensions and the distribution of unexchanged microtubules is focused around the cell nucleus and the centrosome. The most unusual feature of these stable microtu-

bules is that few or none of them are actively growing. Whereas 80% of the dynamic population incorporates subunits within 2 min, <20% of the stable microtubules had incorporated a biotin–tubulin segment in 2 h and this does not seem to increase with time. Since it is likely that stable microtubules arise from dynamic microtubules, we may imagine that the 20% that have incorporated subunits probably incorporated subunits just before they were converted to nongrowing stable microtubules. Thus we can conclude that the cell contains microtubules that are growing, microtubules that are nongrowing and stable, and therefore, the cell must also contain microtubules that are shrinking. Interestingly, when we look at growing microtubules we find that the length of new segments is quite variable (Fig. 2 *A*). In particular, the standard deviation of the growing microtubules measured by us (Schulze and Kirschner, 1986, Fig. 3 *B*) is 41% of the mean. In vitro, the standard deviation of the plus end of a growing microtubule is only 13 or 14% of the mean (calculated from Kristofferson et al., 1986, Table II, for growing plus ends at 0 and 10 min) and this in vitro data should be subject to more experimental error from shearing than the in vivo data. On purely statistical grounds, the standard deviation should be <2% for a microtubule that has grown 2 μm and hence has undergone at least 3,000 subunit additions. In the absence of any obvious experimental source for the variability in vivo and the fact that segments of quite different lengths are found in close proximity in cells (Fig. 2 *B*), we must conclude that microtubule growth rates are in fact variable, and that this may reflect interaction of the ends of the microtubule with other components in the cell.

We would like to be able to estimate how many stable, growing, and shrinking microtubules there are in a cell, and determine their rates of growth and shrinkage. Despite having analyzed over 2,000 injected cells, there are many statistical problems with these estimates. There are also limitations on the spatial resolution obtainable from light microscopy. The most accurate number is that there are ~500 growing microtubules in the average BSC1 cell. We also know that 80% of all microtubules in the cell periphery are growing, which, extrapolating to the whole cell, leads to an estimate of 625 dynamic microtubules (growing plus shrinking). Some of the nongrowing microtubules may be stable, but since fewer than 25% of the stable microtubules are at the cell periphery, we can assume that there are ~100 shrinking microtubules and 500 growing microtubules , a ratio similar to that found at steady state in vitro (Mitchison and Kirschner, 1984*b*). For mass balance to be maintained in this dynamic population, the 500 growing microtubules growing at 3.7 μm/min must be offset by 100 microtubules shrinking at 18.5 μm/min. This extremely rapid rate of depolymerization (~500 subunits/s) is consistent with recently measured rates in vitro (Mitchison and Kirschner, 1984*b*; Horio and Hotani, 1986) and can explain the lack of disassembly intermediates in cells treated with nocodazole (Cassimeris et al., 1986).

There are several ways of estimating the size of the stable population and its half-life, all of which unfortunately are rather imprecise. By 3 h, it is possible to count the number of stable microtubules. By extrapolating the decrease in the average number between 3 and 4 h back to zero time, one estimates 180 stable microtubules with a half-life of 33 min. If one extrapolates between 3 and 5.5 h, one calculates 50 stable microtubules with a half-life of 50 min. If one assumes there are 100 stable microtubules and calculates how many cells one expects with zero microtubules at 4 h, one estimates a half-time of 34 min. Thus with considerable imprecision we estimate that ~15% of the microtubules (100 out of 700) are three to five times more stable than the majority of the dynamic population. It should be remembered that the assumption of two classes of microtubule stability is probably an unwarranted simplification and errors could arise from using the long time points to extrapolate to initial conditions.

The results of nocodazole-sensitivity experiments indicate that stable microtubules are not so stable that they cannot be depolymerized by nocodazole. If nocodazole merely binds to tubulin subunits and prevents their addition to the polymer and if stable microtubules are blocked from both assembly and disassembly reactions at their ends then one might expect them to resist depolymerization. However, in BSC-1 cells stable microtubules have lifetimes only three- to fivefold greater than dynamic microtubules and it is possible that it would be difficult to distinguish small differences in nocodazole sensitivity without a more extensive statistical analysis. It may also be that our assumptions about nocodazole action are incorrect. Nocodazole may interact with the polymer as it is known for instance that colchicine-bound tubulin can form copolymers (Sternlicht and Ringel, 1979). Secondly, it may be that stable microtubules are modified in their dynamics so that they in fact shift often between growth and shrinkage and thus keep a nearly constant length. Blocking growth could then lead to inhibition of the growth phase and consequently rapid net depolymerization. Much more needs to be understood about the action of colchicine and nocodazole to interpret these results.

What makes microtubules differentially stable and what function this serves cannot be answered at present. We can, however, enumerate some of their kinetic properties. The stable microtubules generally show no growth even over long periods of time, although they could be depolymerizing slowly. Since a large majority have not grown over these long periods of time, and there has been a dramatic decrease in their number without an obvious decrease in their length, it suggests that the stable microtubules are not generally depolymerizing slowly but depolymerizing to completion infrequently. We can therefore view stable microtubules as essentially nondynamic, neither growing appreciably nor shrinking appreciably, although short excursions of polymerization and depolymerization cannot be ruled out. Whether stability is achieved by specific capping structures, inhibition of GTP hydrolysis, chemical modification of the entire polymer, lateral binding at the ends, or binding of microtubule-associated proteins along their length is unknown.

The overall shape and distribution of stable microtubules is quite different from the dynamic ones. Stable microtubules are curly and bend in three dimensions and are located primarily around the nucleus and centrosome. This distribution is similar to that reported for detyrosinated tubulin (Gundersen et al., 1984). It is possible that this pericentrosomal location is related to some transport function of microtubules. It could be generated if one imagined that stable microtubules once were dynamic straight microtubules, which after stabilization, were slowly pulled toward the cell center. Evi-

dence of centripetal movement of cortical actin has been presented by Heath (1983). If the microtubules were enmeshed in the cortical actin and the cortical structures moved toward the cell center, the microtubules would end up curly and bent, and they would be of the same overall length as dynamic microtubules. Bent microtubules could also arise if initially straight microtubules were subjected to a force along their length between them and other cytoskeletal elements. The microtubule-based transport molecule, kinesin, would have the proper polarity and in fact in vitro produces kinks in microtubules nucleated from centrosomes (Vale et al., 1985). Kinking and bending would then be a direct consequence of the age of the microtubule and would not necessarily indicate a specific mechanism for differential stabilization. In summary, we find that at any time the 700 microtubules in BSC-1 cells are composed of 500 growing at 4 μm/min, 100 shrinking at ~20 μm/min, and 100 stable microtubules that are essentially nondynamic.

A possible function for both a very dynamic population of microtubules and a spatially distinct set of stable microtubules has been discussed recently (Kirschner and Mitchison, 1986; Kirschner and Schulze, 1987). The major function of the rapid microtubule dynamics would be to explore many different spatial configurations in the cell, so that other mechanisms can choose from among these configurations, ones that serve a functional purpose. In BSC1 cells, we found evidence for a spatially distinguishable subset of microtubules that was also differentially stable. One possible function of this differential stability is to allow for the time-dependent posttranslational modification of these microtubules either by detyrosination or acetylation. This would further differentiate them from the dynamic microtubules. At present, however, there is no known function associated with any of these microtubule subsets. The hypothesis that differential stability of microtubules serves a functional purpose may require testing in more differentiated cells where the function of cell asymmetry is better understood.

We thank Louise Evans for help with the figures, Cynthia Hernandez for preparing the manuscript, and Tim Mitchison for helpful comments on the text.

We thank the National Institutes of General Medical Sciences and the American Cancer Society for supporting this work.

Received for publication 19 July 1986, and in revised form 7 October 1986.

References

Behnke, P., and A. Forer. 1967. Evidence for four classes of microtubules in individual cells. *J. Cell Sci.* 2:169–192.

Bluestein, H. G. 1978. Neurocytotoxic antibodies in serum of patients with systemic lupus erythmatosus. *Proc. Natl. Acad. Sci. USA.* 75:3965–3969.

Bradford, M. M. 1976. A rapid and sensitive method for the quantitation of microgram quantities of protein utilizing the principle of protein-dye binding. *Anal. Biochem.* 72:248–254.

Cassimeris, L. U., P. Wadsworth, and E. D. Salmon. 1986. Dynamics of microtubule depolymerization in monocytes. *J. Cell Biol.* 102:2023–2032.

Graessman, A., M. Graessman, and C. Mueller. 1980. Microinjection of early SV40 DNA fragments and T. Antigen. *Methods Enzymol.* 65:816–825.

Graessman, M., and A. Graessman. 1976. "Early" simian-virus-40 specific RNA contains information for tumor antigen formation and chromatin replication. *Proc. Natl. Acad. Sci. USA.* 73:366–370.

Gundersen, G. G., M. H. Kalnoski, and J. C. Bulinski. 1984. Distinct populations of microtubules: tyrosinated and nontyrosinated alpha tubulin are distributed differently in vivo. *Cell.* 38:779–789.

Heath, J. P. 1983. Direct evidence for microfilament capping of surface receptors on crawling fibroblasts. *Nature (Lond.).* 302:532–534.

Horio, T., and H. Hotani. 1986. Visualization of the dynamic instability of individual microtubules by dark-field microscopy. *Nature (Lond.).* 321:605–607.

Kirschner, M., and T. Mitchison. 1986. Beyond self-assembly: from microtubules to morphogenesis. *Cell.* 45:329–342.

Kirschner, M., and E. Schulze. 1987. Morphogenesis and the control of microtubule dynamics in cells. *Br. Soc. Cell Biol. Symp.* In press.

Kristofferson, D., T. Mitchison, and M. Kirschner. 1986. Direct observation of steady-state microtubule dynamics. *J. Cell Biol.* 102:1007–1019.

LeDizet, M., and G. Piperno. 1986. Cytoplasmic microtubules containing acetylated α-tubulin in *Chlamydomonas reinhardtii*: spatial arrangement and properties. *J. Cell Biol.* 103:13–22.

Mitchison, T., and M. Kirschner. 1984*a*. Microtubule assembly nucleated by isolated centrosomes. *Nature (Lond.).* 312:232–237.

Mitchison, T., and M. Kirschner. 1984*b*. Dynamic instability of microtubule growth. *Nature (Lond.).* 312:237–242.

Mitchison, T., and M. Kirschner. 1985. Properties of the kinetochore in vitro. II. Microtubule capture and ATP-dependent translocation. *J. Cell Biol.* 101:766–777.

Saxton, W. M., D. L. Stemple, R. J. Leslie, E. D. Salmon, M. Zavortink, and J. R. McIntosh. 1984. Tubulin dynamics in cultured mammalian cells. *J. Cell Biol.* 99:2175–2186.

Schulze, E., and M. Kirschner. 1986. Microtubule dynamics in interphase cells. *J. Cell Biol.* 102:1020–1031.

Soltys, B. J., and G. G. Borisy. 1985. Polymerization of tubulin in vivo: direct evidence for assembly onto microtubule ends and from centrosomes. *J. Cell Biol.* 100:1682–1689.

Sternlicht, H., and I. Ringel. 1979. Colchicine inhibition of microtubule assembly via copolymer formation. *J. Biol. Chem.* 254:10540–10550.

Vale, R. D., T. S. Reese, and M. P. Sheetz. 1985. Identification of a novel force-generating protein, kinesin, involved in microtubule-based motility. *Cell.* 42:39–50.

Weingarten, M. D., A. H. Lockwood, S. Hwo, and M. W. Kirschner. 1975. A protein factor essential for microtubule assembly. *Proc. Natl. Acad. Sci. USA.* 72:1858–1862.